JBC Papers in Press. Published on October 19, 2007 as Manuscript M701021200
The latest version is at http://www.jbc.org/cgi/doi/10.1074/jbc.M701021200

PARP-2 controls adipocyte differentiation and adipose tissue function through the regulation of the activity of the RXR/PPARγ heterodimer

Péter Bai[1,3], Sander M. Houten[2,4], Aline Huber[1], Valérie Schreiber[1], Mitsuhiro Watanabe[2], Borbála Kiss[1], Gilbert de Murcia [1], Johan Auwerx[2,5] and Josiane Ménissier-de Murcia[1]

Running title: PARP-2 as a cofactor of PPARγ

[1]Département Intégrité du Génome, UMR 7175 du CNRS, Ecole Supérieure de Biotechnologie de Strasbourg, BP 10413, 67412 Illkirch, France
[2]Institut de Génétique et Biologie Moléculaire et Cellulaire, 1 Rue Laurent Fries, BP 10142, 67404 Illkirch, France
[3]Department of Medical Chemistry, University of Debrecen, Debrecen, Hungary
[4]Laboratory Genetic Metabolic Diseases, Academic Medical Center, Amsterdam, The Netherlands
[5]Institut Clinique de la Souris, 1 Rue Laurent Fries, BP 10142, 67404 Illkirch, France

Whom correspondence should be sent to: Peter Bai, Ph.D., University of Debrecen, MHSC, Department of Medical Chemistry, 4032 Debrecen, Nagyerdei krt. 98., Pf. 7., Hungary, Tel. +36 52 412 345; Fax. +36 52 412 566, E-mail: baip@dote.hu

The peroxisome proliferator activated receptor-γ (PPARγ, NR1C3) in complex with the retinoid X receptor (RXR) plays a central role in white adipose tissue (WAT) differentiation and function, regulating the expression of key WAT proteins. In this report we show that poly(ADP-ribose) polymerase-2 (PARP-2), also known as an enzyme participating in the surveillance of the genome integrity, is a member of the PPARγ/RXR transcription machinery. PARP-2$^{-/-}$ mice accumulate less WAT, characterized by smaller adipocytes. In the WAT of PARP-2$^{-/-}$ mice the expression of a number of PPARγ target genes is reduced despite the fact that PPARγ1 and γ2 are expressed at normal levels. Consistent with this, PARP-2$^{-/-}$ mouse embryonic fibroblasts fail to differentiate to adipocytes. In transient transfection assays, PARP-2 siRNA decreases basal activity and ligand-dependent activation of PPARγ, whereas PARP-2 overexpression enhances the basal activity of PPARγ, although it does not change the maximal ligand-dependent activation. In addition, we show a DNA-dependent interaction of PARP-2 and PPARγ/RXR heterodimer by chromatin immunoprecipitation. In combination, our results suggest that PARP-2 is a novel cofactor of PPARγ activity.

Adipose tissue is composed of adipocytes that store energy in the form of triglycerides. Excessive accumulation of white adipose tissue (WAT) leads to obesity, while its absence leads to lipodystrophic syndromes. The peroxisome proliferator-activated receptor-γ (PPARγ, NR1C3) is the main protein orchestrating the differentiation and function of WAT, as evidenced by the combination of *in vitro* studies, the analysis of mouse models and the characterization of patients with mutations in the human PPARγ gene (1), (2). PPARγ acts as heterodimer with the retinoid X receptor (RXR) (3). The PPARγ/RXR receptor dimer is involved in the transcriptional control of energy, lipid, and glucose homeostasis (4); (5). The actions of PPARγ are mediated by two protein isoforms, the widely expressed PPARγ$_1$ and adipose tissue-restricted PPARγ$_2$, both produced from a single gene by alternative splicing and differing only by an additional 28 amino acids in the NH_2-terminus of PPARγ$_2$ (6); (3).

PPARγ is activated by binding of small lipophilic ligands, mainly fatty acids, derived from nutrition or metabolic pathways, or synthetic agonists, like the anti-diabetic thiazolidinediones (2), (7); (8). Docking of these ligands in the ligand binding pocket alters the conformation of PPARγ, resulting in transcriptional activation subsequent to the release of corepressors and the recruitment of coactivators. Many corepressors and coactivators have been described such as the nuclear receptor corepressor (N-CoR) and the steroid receptor coactivators (SRCs), also known as p160 proteins (9); (10) (11). These corepressors and coactivators determine transcriptional activity by altering chromatin structure via enzyme such as histone deacetylases (HDACs) and histone acetyltransferases (CBP/p300). Other mechanisms include DNA-methylation, ATP-dependent remodeling, protein phosphorylation, SUMOylation and ubiquitinylation and poly(ADP-ribosyl)ation.

Poly(ADP-ribose) polymerase-2 (PARP-2) was described by Ame *et al* in 1999 as a 66.2 kDa nuclear protein with poly(ADP-ribosyl)ating activity. Through its DNA-binding domain in the N-terminus (amino acid 1-62), PARP-2 can bind to DNase I treated DNA and to aberrant DNA forms and its subsequent activation results in poly(ADP-ribose) polymer (PAR) formation (12). According to the general scheme of PARP activation, the active enzyme catalyses the polymerisation of PAR onto different acceptor proteins and itself using NAD^+ as a substrate (13). PARP-2 shares a similar catalytic domain (amino acid 202-593) as poly(ADP-ribose) polymerase-1 (PARP-1) (14), the founding member of the PARP family, though PARP-2 has a smaller reaction velocity compared to PARP-1 (12).

PARP-2 has multiple *in vivo* functions comprising DNA surveillance and DNA repair processes (reviewed in (15)), spermatogenesis (16), (17), inflammation and oxidative injury (18), (19), (20). Most of these functions are accomplished through protein-protein interactions. In PARP-2, the interaction platforms can be mapped to the DNA-binding domain and to the domain E (amino acid 63-202) (21); (22); (23); (24); (25). A role for PARP-2 in the regulation of transcription has already been described. In lung epithelial cells PARP-2 interacts with thyroid transcription factor-1 (TTF1). TTF1 is a homeodomain-containing transcription factor of the Nkx-2 family. In these cells, PARP-2 regulates the expression of the surfactant protein-B by affecting TTF1 activity (25). In this study we show that PARP-2 affects the transcriptional activity of PPARγ both *in vitro* and *in vivo*.

EXPERIMENTAL PROCEDURES

Materials - All chemicals were from *Sigma-Aldrich* (St. Louis, MO, USA) unless stated otherwise.

Animals - PARP-$2^{-/-}$ mice and their wild-type (WT) littermates (26) coming from heterozygous crossings were used. Mice were housed separately, had ad libitum access to water and chow, and were kept under a 12 h dark-light cycle. The animals were killed at the age of 7 months by cervical dislocation after 4 hours of fasting and tissues were collected.

Cell culture - 3T3-L1 cells were maintained in DMEM (*Invitrogen*, Carlsbad, CA), 10% NCS (*Invitrogen*), Gentamicine (*Invitrogen*) and HEK and mouse embryonic fibroblasts (MEFs) in DMEM, 10% FCS (*Adgenix*, Voisins le Bretonneux, France), Gentamicine (*Invitrogen*). The 3T3-L1 cells were maintained subconfluent.

MEF preparation and differentiation - MEFs were prepared from embryos as described elsewhere (26;26). For the differentiation studies $4x10^5$ MEFs were seeded in 12 well plates and were maintained in DMEM, 10% FCS. The medium was changed every 2 days until confluence. The cells were maintained at confluency for 2 days. Cells were then differentiated in DMEM, 10% NCS, 5 µM troglitazone (TZD), 5 µM dexamethasone (Dex), 500 µM IBMX and 10 µg/ml insulin (later defined as differentiation mix), while the control cells received DMEM, 10% FCS and DMSO as vehicle. The medium with the differentiation mix

was replaced every 2 days and the cells were differentiated for 8 days. Control cells after confluency were cultured in DMEM+10% FCS containing only vehicle (DMSO 0.21%).

DNA constructs - To create an siRNA expressing construct, double stranded oligonucleotides were cloned into the pSuper vector (for sequences see Table 1.) (27). The oligonucleotides siPARP-2sense and siPARP-2antisense (containing the siRNA sequence), as well as the control scrPARP-2sense and scrPARP-2antisense (scrambled version of the siRNA sequence) respectively were annealed in annealing buffer (150mM NaCl, 1mM EDTA, 50 mM Hepes pH. 8.0). The resulting duplexes carried *Bgl*II and *Hind*III sites and were cloned into pSuper using these sites resulting in pSuper-siPARP-2 (oligos siPARP-2sense + siPARP-2antisense) and pSuper-scrPARP-2 (oligos scrPARP-2sense + scrPARP-2antisense). An *Eco*RV/*Sma*I fragment encoding mouse PARP-2 was isolated from pBC-mPARP-2 ((23)) and inserted into the *Sna*BI site of pBABEpuro (*Addgene*, Cambridge, MA), giving the pBABE-mPARP-2 vector. All other constructs pGL3-$(J_{wt})_3$TKluc reporter construct (28), pSG-PPARγ_2, (3), pSG5-PPARα (29), pSG5-PPARβ (30), pCMX-ERβ, and vitellogeninA2-ERE-TKLuc (ER-luc) (31) were described before. The pCMV-βGal was used to control the transfection efficiency.

Transfections - Transfections were preformed either by the BES buffered saline (BBS) method (26) or by JetPei (*Polyplus Transfections*, Illkirch, France).

Luciferase activity measurement - $3x10^5$ HEK cells were seeded in 6 well plates and were transfected with pSuper-siPARP-2, pSuper-scrPARP-2, pBabe or pBabe-PARP-2 using the BBS method. Two days later the cells were once more transfected with the constructs mentioned above. Cells were transfected 24 hours later with 0.6 µg pSuper-siPARP-2/pSuper-scrPARP-2/pBabe/pBabe-PARP-2; 0.4 µg β–galactosidase expression plasmid; 1 µg pSG-PPARα/pSG-PPARβ/ pSG-PPARγ_2/pCMX-ERβ expression vector; 1 µg PPAR- /ER-responsive construct. Six hours after transfection, cells were scraped and luciferase activity was determined. For the determination of PPAR activity, just before transfection, cells were washed in serum-free DMEM medium, and the transfection was carried out in DMEM + 10% fat-free serum. As ligand we used, fenofibrate (FF) (50 µM), mono-ethyl-hexyl-phthalate (MEHP) (100 µM), TZD (5µM), and β-estradiol (10 µM). After 6 hours of transfection cells were washed with PBS, scraped and stored at –80^{o}C. Luciferase assay was carried out by standard procedures. Luciferase activity was expressed as luciferase activity/β-galactosidase activity.

Nile-Red flow cytometry - To assess the extent of MEF differentiation, cytosolic triglyceride content was assessed by determining Nile-Red uptake (modified from (32)) followed by flow cytometry using a FACSCalibur machine (*BD, San Diego, CA, USA*). Cells were harvested by adding Trypsin-EDTA and the detached cells were stained with Nile-Red (20 µg/ml, 5 min.). Cells were subjected to flow cytometric analysis with 10000 events collected for each sample, each measurement point was repeated in 4 parallel replicates. Samples for each cell line were normalized against the non-differentiated cells of the same line. The rate of differentiation was expressed as the percentage of the differentiated cells vs. total number of cells.

SDS-PAGE - Western blot - Cells were lysed in lysis buffer (50 mM Tris, 500 mM NaCl, 1 mM EDTA, 1% NP40, 1 mM PMSF, protease inhibitor cocktail, pH 8.0). Proteins were separated by SDS-PAGE and transferred onto nitrocellulose membranes. For the detection of PARP-2, a polyclonal rabbit antibody was used 1:2000, *Alexis*, Lausen, Switzerland) and actin was as detected using a rabbit polyclonal antibody (*Sigma*, 1:200). The secondary antibody was IgG-peroxidase conjugate (*Sigma*, 1:10000). Reactions were developed by enhanced chemiluminescence (*Amersham*, Little Chalfont, UK).

Total RNA preparation, reverse transcription and qPCR - Total RNA was prepaired using Trizol (*Invitrogen*)

according to the manufacturer's instructions. RNA was treated with DNase and 2 μg RNA was used for reverse transcription (RT). cDNA was purified on Qiaquick PCR cleanup columns (*Qiagen*, Valencia, CA, USA). 50X diluted cDNA was used for quantitative PCR (qPCR) reactions. The qPCR reactions were preformed using the LightCycler system (*Roche*, Basel, Switzerland) and a qPCR supermix (*Qiagen*) with the primers summarized in Table 2.

Chromatin immunoprecipitation - Chromatin immunoprecipitation was performed according to (33) on 3T3-L1 cells using α-PARP-2, α-PPARγ$_2$ (*Alexis,* Lausen, Switzerland), and α-MMP9 (*Santa Cruz*, Santa Cruz, CA) antibodies. We used also a no antibody control. The chromatin fragments collected upon precipitation with the above antibodies were amplified using promoter-specific primers by qPCR. For the analysis of the coding sequence the same qPCR primer set was used as the one for the quantitation of the given gene. The respective primers are listed in Table 2 and Table 3. The results were normalized for the signal of the input and were expressed as a percentage of the aP2 signal with the PARP-2 antibody.

For the testing of the K19 primer set we used non-confluent 3T3-L1 cells transfected with pCMX-ERβ. Chromatin immunoprecipitation was performed using the α-ERβ, (*Santa Cruz*), as controls we used an α-MRE11 (*Santa Cruz*) and a no antibody control. The chromatin fragments collected upon precipitation with the above antibodies were amplified using K19 promoter-specific primers by qPCR.

Microscopy - Formaldehyde-fixed, paraffin-embedded sections (7 μm) were made from WAT samples and were stained with haematoxylin-eosine (HE). The same sections were stained with a biotin-conjugated F4/80 antibody (*Serotec*, Raleigh, NC, USA, 1:100 dilution) and the bound primary antibodies were detected using streptavidin-perxidase (Vector ABC kit) and diamino-benzidine as chromogenic substrate. Terminally differentiated MEFs were stained by Oil-Red O as described elsewhere.

Triglyceride measurement - Triglyceride content of the MEFs were determined using commercially available Sigma kit according to the manufacturer's instructions.

Statistical analysis - Significance was analyzed by Student`s t-test. Error bars represent +/- SEM, unless noted otherwise.

RESULTS

In vivo dysfunction of the PPARγ/RXR heterodimer in the white adipose tissue of PARP-2$^{-/-}$ mice. The different fat-depots (epididymal-, mesenteric- and inguinal- and the interscapular brown adipose tissue associated WAT were measured in 7 month old PARP-2$^{-/-}$ mice and their wild type littermates. A proportional loss of the weight of all adipose tissue depots was observed in the PARP-2$^{-/-}$ mice (Fig. 1A).

Histological examination of the PARP-2$^{-/-}$ epididymal WAT showed adipocytes with reduced and irregular size. This tissue contained diluted capillaries, indicative of inflammation, which was confirmed by a faint staining with the macrophage-specific F4/80 antibody in the PARP-2$^{-/-}$ (Fig. 1B, 1C) and the macroscopic appearance of the WAT (Fig.1A). The F4/80 positive cells were present in the vicinity of the blood vessels.

To identify the molecular changes that contribute to the decreased fat accumulation and abnormal adipocyte morphology we determined the expression of the PPARγ target genes, TNFα and hormone sensitive lipase (HSL) by RT-qPCR in the epididymal WAT.

TNFα expression was undetectable in 8 of the 22 mice used for this study (4

out of 14 PARP-$2^{+/+}$ and 4 out of 8 PARP-$2^{-/-}$). In the TNFα positive mice, expression levels were not different, ruling out a major role for inflammation in the adipose tissue dysfunction in PARP-$2^{-/-}$ mice. The expression level of HSL, which is responsible for lipolysis, was also not different between the 2 genotypes. The expression of several PPARγ target genes, however, was markedly decreased. These include genes involved in chylomicron and VLDL triglyceride hydrolysis (lipoprotein lipase; LPL), FFA uptake (CD36), *de novo* fatty acid synthesis (fatty acid synthase; FAS) and endocrine signaling (leptin, adiponectin) (Fig. 1D). Interestingly, no difference was detected in $PPAR\gamma_1$ and $PPAR\gamma_2$ mRNA levels between the different genotypes.

MEF differentiation is affected by PARP-2 ablation. We next aimed to determine whether MEFs differentiation towards adipocytes was affected by the PARP-2 deletion. Differentiation of PAPR-$2^{-/-}$ MEFs into adipocytes was decreased as judged by Oil-Red O staining, determination of lipid content and Nile-red staining followed by FACS analysis (Fig. 2A).

The expression of genes involved in adipocyte differentiation and function such as $PPAR\gamma_1$ and $PPAR\gamma_2$ were decreased in the PARP-$2^{-/-}$ MEFs (34). Since the PPARγ transcripts are primarily present in the differentiated cells, these data confirm that PARP-$2^{-/-}$ cells differentiate less into adipocytes. The expression of PPARγ target genes, such as LPL, FAS, leptin, adiponectin and adipocyte fatty acid-binding protein 2 (aP2), were decreased in parallel (Fig. 2B).

PARP-2 expression modulates transactivation of PPARs. To measure whether changes in PARP-2 expression affect PPAR transactivation, we used HEK 293 cells transfected with a $PPAR\gamma_2$ expression vector and a PPARγ responsive luciferase construct. In these experiments we modulated the expression of PARP-2 expression by overexpression and siRNA depletion. For the siRNA depletion of PARP-2 we used the pSuper-siPARP-2 construct, whereas for PARP-2 overexpression we used the pBabe-PARP-2. The pSuper-scrPARP-2 and the empty pBabe vector served as the respective controls. PARP-2 levels were assessed by Western blotting using a PARP-2 specific antibody. For both constructs, the cells were transfected twice, on day 0 and on day 2. On day 3, the specific siRNA decreased PARP-2 protein levels significantly, whereas the scrambled PARP-2 siRNA did not alter the PARP-2 levels. A strong increase in PARP-2 protein was observed on day 3 of the overexpression experiment (Fig 3).

PARP-2 depletion diminished the basal PPARγ activity and abrogated receptor activation by its synthetic ligand, troglitazone. Conversely, PARP-2 overexpression induced by 3-fold the basal PPARγ activity, although it does not significantly change the ligand-dependent activation by TZD (Fig. 4A). To verify whether this effect of PARP-2 was specific for PPARγ, we performed similar experiments for the related nuclear receptors PPARα (NR1C1) and PPARβ (NR1C2), and the unrelated estrogen receptor β (ERβ, NR3A2). Interestingly, siRNA depletion of PARP-2 increased the basal activity of both PPARα and β (Figure 4B, C). PARP-2 overexpression did not affect PPARβ, but increased PPARα activity. The activation of PPARα and β with FF and MEHP, respectively, was not modified by the modulation of PARP-2 expression. In addition, neither PARP-2 depletion, nor PARP-2 overexpression had an effect on the basal or ligand-induced activity of ERβ (Fig. 4D). Combined these results indicate specificity of the PARP-2-dependent effect on PPARγ.

PARP-2 is the member of the RXR-PPARγ transcription complex. To demonstrate an interaction between PPARγ and PARP-2 we used ChIP assays. To precipitate chromatin from undifferentiated 3T3-L1 cells we used antibodies against PARP-2 and $PPAR\gamma_2$. An anti-matrix metalloproteinase-9 (MMP-9) antibody and a no antibody sample served as negative controls. We used qPCR to amplify the promoters of the aP2 (6) and CD36 (35) as promoters driven by PPARγ, and keratin-19 (K19), as a non-related,

ERβ-regulated promoter (36). PARP-2 and PPARγ gave a strong signal on PPARγ-regulated promoters. These signals were significantly higher compared to the signal from the K-19 promoter (Fig. 5A). We also performed qPCR reactions to cover the coding sequences of aP2 using the chromatin fragments obtained in the ChIP experiments. The signal of PARP-2 and PPARγ coding sequences in the immunoprecipitates was strongly decreased compared to the signal of the corresponding promoter. Apparently, both PARP-2 and PPARγ are present on the PPARγ-driven promoters, but not in the coding sequence (Fig. 5B). In addition, our results suggest that PARP-2 possesses specificity towards the PPARγ-driven promoters since the signal from ERβ-driven K-19 promoter was significantly lower than that from PPARγ-driven promoters.

Despite of the huge difference in the signal of the specific promoters and the non-specific regions (K19 promoter, coding sequence) we observed some background signal from the non-specific region. It is likely that this represents the real presence of PARP-2 in these regions, which is probably linked to the formaldehyde-induced DNA damage.

To provide proof that the interaction of ERβ with the K19 promoter is basically detectable we complemented 3T3-L1 cells with ERβ and we performed ChIP probing with the K19 primer set. To precipitate chromatin from ERβ-complemented 3T3-L1 cells we used an antibody against ERβ, an anti-MRE11 antibody and a no antibody sample served as negative controls. The precipitate of the ERβ-specific antibody gave significantly higher signal then the non-specific MRE11 (2.7 fold increase) as well as with the no antibody control (6.1 fold increase) proving that the K19 primer pair is capable of detecting the K19 promoter if present in the precipitate (Fig. 5C).

DISCUSSION

PPARγ plays an important role in adipose tissue differentiation and function. In PARP-2 knockout mice we have identified a defect of adipose tissue function and a decrease of adipocyte differentiation. *In vivo*, the adipose tissue depots had smaller weight and histologically showed an adipodegenerative phenotype.

We have detected a mild inflammation in the WAT of the PARP-2$^{-/-}$ mice. The capillaries were dilated and we have detected F4/80 positive cells in the vicinity of the capillaries suggesting the presence of macrophages. The areas more distant from the capillaries are devoid of staining. Similar coloration was not observed in the WAT of the wild type mice. Activated macrophages and adipocytes may secrete proinflammatroy cytokines, such as TNFα that may induce adipocyte cell death (37). Since TNFα expression was not detectable in many mice and if it was detected, its expression was not significantly increased by the absence of PARP-2, it is less likely that inflammation is a leading cause of the adipodegeneration in the PARP-2$^{-/-}$ mice. It is also unlikely that increased lipolysis may contribute to the phenotype in the PARP-2$^{-/-}$ mice, since there was no difference in the expression of HSL between the wild-type and PARP-2$^{-/-}$ mice.

We did observe decreased expression of multiple PPARγ target genes involved in adipocyte function. Expression of both PPARγ isoforms was normal, suggesting effects on PPARγ/RXR transactivation. *In vitro*, the differentiation of the PARP-2$^{-/-}$ MEFs into adipocytes was delayed when compared with the differentiation of wild-type MEFs. At the end of the differentiation the expression of both PPARγ$_1$ and PPARγ$_2$ was decreased in the PARP-2$^{-/-}$ cells indicating the lack of differentiation. Similarly, the expression of the PPARγ target genes was decreased.

In transfection assays, the ablation of PARP-2 results in the diminution, whereas PARP-2 overexpression raises transactivation by PPARγ. The effect of PARP-2 seems specific for PPARγ, since opposite or no effects were observed for the related PPARα and PPARβ, and the non related ERβ.

PARP-2 achieves these activities because it is part of the PPARγ/RXR

transcription complex as shown by ChIP assays, suggesting that PARP-2 could act as a PPARγ/RXR receptor cofactor.

Both members of the PPARγ – RXR nuclear receptor dimer might be the effector behind the phenotype of the PARP-$2^{-/-}$ mice. If PARP-2 would influence directly RXR all PPAR isoforms should respond the same way to the modulation of PARP-2 expression. PPARγ was differentially regulated when compared with PPARα and β, suggesting that PARP-2 acts on PPARγ.

Our report comprises *in vitro* data and gives first time *in vivo* evidence that PARP-2 may be considered a cofactor of nuclear receptor transcription.

PARP-2 is a multidomain protein with multiple functions. These functions comprise DNA repair (reviewed in (15)), spermatogenesis (16), (17), T-cell development (38), inflammation and oxidative injury (18), (19), (20). Most of these functions are accomplished through protein-protein interactions. The N-terminus, with the following domain E are apparently important protein-protein interaction domains, serving as interaction platform for TRF-2 (39), B23 (22), PARP-1, XRCC1, DNA polymerase β (23), and TTF1 (25). PARP-2 also homodimerises with itself through its domain E (23).

PARP-1 has been described as a cofactor for numerous transcription factors (reviewed in (40) and (25)), including for some members of the nuclear receptor family, such as the progesterone receptor (41), RXR (42); (43) androgen receptor (44) and the thyroid receptor (42). A recent study, based on *in vitro* results, suggested that PARP-2 acts as a cofactor of a homeodomain-containing transcription factor, TTF1 that belongs to the Nkx-2 family. Binding of PARP-2 through its E-domain to the C-terminus of TTF1 regulates the expression of the surfactant protein-B in lung epithelial cells. TTF1-mediated transcription encompasses similar mechanisms including chromatin modification, and involves some of the same cofactors such as the SRCs as described for PPARγ-coupled transcription. This suggests that similar molecular mechanisms exist both in the case of PPARγ- and TTF1-mediated transcription (25). Our results hence confirm the observation of Maeda and colleagues, that PARP-2 is a cofactor of some transcription factors, and extend these conclusions by showing that PARP-2 is involved in nuclear receptor-mediated transcriptional control *in vivo*. Recent evidence has suggested that the interaction between PARP-1 and the promoter of target gene could be mediated via double strand breaks, which are produced by activation of a nuclear receptor followed by the unwinding of DNA by topoisomerase II (45). Our results do provide evidence that interaction with DNA is important for the interaction between PPARγ and PARP-2. ChIP assays that depend on DNA binding show strong interaction. In contrast, immunoprecipitation experiments performed on cell extracts showed only a weak interaction between PARP-2 and PPARγ (data not shown), which was abrogated by low concentrations of NP40 (>0.1%). Furthermore, like is the case for PARP-1, the NH_2-terminus of PARP-2, comprising its DNA-binding domain, seems also to play the most important role in the interaction with PPARγ. Consistent with this observation a nuclear receptor-binding consensus sequence (^{113}LIQLL^{117}) was present in the E domain of PARP-2.

Concerning the mode of action of PARP-2, it is possible that not only the physical presence but also the activity of PARP-2 is necessary for the nuclear receptor function. Poly(ADP-ribosyl)ation is reported to increase throughout the differentiation process of 3T3-L1 cells (46). Interestingly this poly(ADP-ribosyl)ation activity is not completely inhibited by PARP-1 depletion (47), suggesting the involvement of other member(s) of the PARP family, such as PARP-2. Indeed both PARP-1 and PARP-2 are reported to poly(ADP-ribosyl)ate histones (13). Similarly to histone acetylation, poly(ADP-ribosyl)ation of the high mobility group of proteins and histones, loosens chromatin structure enabling transcription initiation (48). Consistent with this line of thinking, there is molecular and *in vivo* evidence that the

enzymatic activity of PARP-1 is necessary for efficient gene transcription and inhibition of PARP activity impairs the transcription of a number of different genes, including different chemokines and inflammation-related genes (e.g. iNOS, TNFα, ICAM-1, IL-8, MIP-1α, IL–12) (49), (40), (50).

PARP-2 specifically occupies the promoter of PPARγ target genes, since it bound efficiently to the regulatory sequence, whereas binding to the corresponding coding sequences was strongly decreased. Despite this rather specific binding, we observed a background signal rising most likely from non-coding regions or from non-PPARγ – dependent promoters, such as that of the K19 gene, which is under the control of ERβ. When comparing the specific to the above mentioned non-specific signal it is at least 10-100 fold increased, which can be considered as a significant difference. It is likely that the non-specific presence of PARP-2 on the K19 promoter and in the non-coding regions is explained by the fact that PARP-2 binds to the DNA-damage sites created by the formaldehyde treatment during the crosslinking of the cells. The crosslinking-related DNA damage is present throughout the entire genome, equally affecting coding regions and promoters, thus theoretically providing a background signal throughout the genome.

The present study indicates that PARP-2 modulates the activity of PPARγ/RXR nuclear receptor complex, a key transcription factor involved in the pathogenesis of several important diseases such as obesity, insulin resistance, type II diabetes atherosclerosis and lipodystrophy. Since many of these diseases affect a large part of the population and have high costs to society, our data linking the activation of PPARγ and PARP-2, open up the possibility to modulate PPARγ activity via PARP-2. It is therefore tempting to speculate that the various PARP inhibitors that are currently being developed and being tested in clinical trials (51) could also be useful in the metabolic disease arena.

REFERENCES

1. Gurnell, M. (2005) *Best. Pract. Res. Clin. Endocrinol. Metab.* **19,** 501-523

2. Knouff, C. and Auwerx, J. (2004) *Endocr. Rev.* **25,** 899-918

3. Fajas, L., Auboeuf, D., Raspe, E., Schoonjans, K., Lefebvre, A. M., Saladin, R., Najib, J., Laville, M., Fruchart, J. C., Deeb, S., Vidal-Puig, A., Flier, J., Briggs, M. R., Staels, B., Vidal, H., and Auwerx, J. (1997) *J. Biol. Chem.* **272,** 18779-18789

4. Evans, R. M., Barish, G. D., and Wang, Y. X. (2004) *Nat. Med.* **10,** 355-361

5. Cock, T. A., Houten, S. M., and Auwerx, J. (2004) *EMBO Rep.* **5,** 142-147

6. Tontonoz, P., Hu, E., Graves, R. A., Budavari, A. I., and Spiegelman, B. M. (1994) *Genes Dev.* **8,** 1224-1234

7. Rosen, E. D. and Spiegelman, B. M. (2001) *J. Biol. Chem.* **276,** 37731-37734

8. Lehrke, M. and Lazar, M. A. (2005) *Cell.* **123,** 993-999

9. McKenna, N. J. and O'Malley, B. W. (2002) *Cell.* **108,** 465-474

10. Rosenfeld, M. G., Lunyak, V. V., and Glass, C. K. (2006) *Genes Dev.* **20,** 1405-1428

11. Feige, J. N. and Auwerx, J. (2007) *Trends Cell Biol.* **17,** 292-301

12. Ame, J. C., Rolli, V., Schreiber, V., Niedergang, C., Apiou, F., Decker, P., Muller, S., Hoger, T., Menissier-de Murcia, J., and de Murcia, G. (1999) *J. Biol. Chem.* **274,** 17860-17868

13. Schreiber, V., Dantzer, F., Ame, J. C., and de Murcia, G. (2006) *Nat. Rev. Mol. Cell Biol.* **7,** 517-528

14. Oliver, A. W., Ame, J. C., Roe, S. M., Good, V., de Murcia, G., and Pearl, L. H. (2004) *Nucleic Acids Res.* **32,** 456-464

15. Huber, A., Bai, P., Menissier-de Murcia, J., and de Murcia, G. (2004) *DNA Repair (Amst).* **3,** 1103-1108

16. Tramontano, F., Di, M. S., and Quesada, P. (2005) *J. Cell Biochem.* **94,** 58-66

17. Dantzer, F., Mark, M., Quenet, D., Scherthan, H., Huber, A., Liebe, B., Monaco, L., Chicheportiche, A., Sassone-Corsi, P., de Murcia, G., and Menissier-de Murcia, J. (2006) *Proc. Natl. Acad. Sci. U. S. A.* **103,** 14854-14859

18. Kofler, J., Otsuka, T., Zhang, Z., Noppens, R., Grafe, M. R., Koh, D. W., Dawson, V. L., Menisser-de Murcia, J., Hurn, P. D., and Traystman, R. J. (2006) *J. Cereb. Blood Flow Metab.* **26,** 135-141

19. Mota, R. A., Sanchez-Bueno, F., Saenz, L., Hernandez-Espinosa, D., Jimeno, J., Tornel, P. L., Martinez-Torrano, A., Ramirez, P., Parrilla, P., and Yelamos, J. (2005) *Lab Invest.* **85,** 1250-1262

20. Popoff, I., Jijon, H., Monia, B., Tavernini, M., Ma, M., McKay, R., and Madsen, K. (2002) *J. Pharmacol. Exp. Ther.* **303,** 1145-1154

21. Dantzer, F., Giraud-Panis, M. J., Jaco, I., Ame, J. C., Schultz, I., Blasco, M., Koering, C. E., Gilson, E., Menissier-de, M. J., de, M. G., and Schreiber, V. (2004) *Mol. Cell Biol.* **24,** 1595-1607

22. Meder, V. S., Boeglin, M., de, M. G., and Schreiber, V. (2005) *J. Cell Sci.* **118,** 211-222

23. Schreiber, V., Ame, J. C., Dolle, P., Schultz, I., Rinaldi, B., Fraulob, V., Menissier-de Murcia, J., and de Murcia, G. (2002) *J. Biol. Chem.* **277,** 23028-23036

24. Saxena, A., Wong, L. H., Kalitsis, P., Earle, E., Shaffer, L. G., and Choo, K. H. (2002) *Hum. Mol. Genet.* **11,** 2319-2329

25. Maeda, Y., Hunter, T. C., Loudy, D. E., Dave, V., Schreiber, V., and Whitsett, J. A. (2006) *J. Biol. Chem.* **281,** 9600-9606

26. Menissier-de Murcia, J., Ricoul, M., Tartier, L., Niedergang, C., Huber, A., Dantzer, F., Schreiber, V., Ame, J. C., Dierich, A., LeMeur, M., Sabatier, L., Chambon, P., and de Murcia, G. (2003) *EMBO J.* **22,** 2255-2263

27. Brummelkamp, T. R., Bernards, R., and Agami, R. (2002) *Science.* **296,** 550-553

28. Vu-Dac, N., Schoonjans, K., Kosykh, V., Dallongeville, J., Fruchart, J. C., Staels, B., and Auwerx, J. (1995) *J. Clin. Invest.* **96,** 741-750

29. Issemann, I. and Green, S. (1990) *Nature.* **347,** 645-650

30. Amri, E. Z., Bonino, F., Ailhaud, G., Abumrad, N. A., and Grimaldi, P. A. (1995) *J. Biol. Chem.* **270,** 2367-2371

31. Tremblay, G. B., Tremblay, A., Copeland, N. G., Gilbert, D. J., Jenkins, N. A., Labrie, F., and Giguere, V. (1997) *Mol. Endocrinol.* **11,** 353-365

32. Maquoi, E., Munaut, C., Colige, A., Collen, D., and Lijnen, H. R. (2002) *Diabetes.* **51,** 1093-1101

33. Balint, B. L., Szanto, A., Madi, A., Bauer, U. M., Gabor, P., Benko, S., Puskas, L. G., Davies, P. J., and Nagy, L. (2005) *Mol. Cell Biol.* **25,** 5648-5663

34. Saladin, R., Fajas, L., Dana, S., Halvorsen, Y. D., Auwerx, J., and Briggs, M. (1999) *Cell Growth Differ.* **10,** 43-48

35. Motojima, K., Passilly, P., Peters, J. M., Gonzalez, F. J., and Latruffe, N. (1998) *J. Biol. Chem.* **273,** 16710-16714

36. Kian Tee, M., Rogatsky, I., Tzagarakis-Foster, C., Cvoro, A., An, J., Christy, R. J., Yamamoto, K. R., and Leitman, D. C. (2004) *Mol. Biol. Cell.* **15,** 1262-1272

37. Prins, J. B., Niesler, C. U., Winterford, C. M., Bright, N. A., Siddle, K., O'Rahilly, S., Walker, N. I., and Cameron, D. P. (1997) *Diabetes.* **46,** 1939-1944

38. Yelamos, J., Monreal, Y., Saenz, L., Aguado, E., Schreiber, V., Mota, R., Fuente, T., Minguela, A., Parrilla, P., de Murcia, G., Almarza, E., Aparicio, P., and Menissier-de Murcia, J. (2006) *EMBO J.* **25,** 4350-4360

39. Dantzer, F., Giraud-Panis, M. J., Jaco, I., Ame, J. C., Schultz, I., Blasco, M., Koering, C. E., Gilson, E., Menissier-de, M. J., de, M. G., and Schreiber, V. (2004) *Mol. Cell Biol.* **24,** 1595-1607

40. Virag, L. and Szabo, C. (2002) *Pharmacol. Rev.* **54,** 375-429

41. Sartorius, C. A., Takimoto, G. S., Richer, J. K., Tung, L., and Horwitz, K. B. (2000) *J. Mol. Endocrinol.* **24,** 165-182

42. Pavri, R., Lewis, B., Kim, T. K., Dilworth, F. J., Erdjument-Bromage, H., Tempst, P., de, M. G., Evans, R., Chambon, P., and Reinberg, D. (2005) *Mol. Cell.* **18,** 83-96

43. Miyamoto, T., Kakizawa, T., and Hashizume, K. (1999) *Mol. Cell Biol.* **19,** 2644-2649

44. Mayeur, G. L., Kung, W. J., Martinez, A., Izumiya, C., Chen, D. J., and Kung, H. J. (2005) *J. Biol. Chem.* **280,** 10827-10833

45. Ju, B. G., Lunyak, V. V., Perissi, V., Garcia-Bassets, I., Rose, D. W., Glass, C. K., and Rosenfeld, M. G. (2006) *Science.* **312,** 1798-1802

46. Janssen, O. E. and Hilz, H. (1989) *Eur. J. Biochem.* **180,** 595-602

47. Smulson, M. E., Kang, V. H., Ntambi, J. M., Rosenthal, D. S., Ding, R., and Simbulan, C. M. (1995) *J. Biol. Chem.* **270,** 119-127

48. Kim, M. Y., Zhang, T., and Kraus, W. L. (2005) *Genes Dev.* **19,** 1951-1967

49. Nirodi, C., NagDas, S., Gygi, S. P., Olson, G., Aebersold, R., and Richmond, A. (2001) *J. Biol. Chem.* **276,** 9366-9374

50. Oliver, F. J., Menissier-de Murcia, J., Nacci, C., Decker, P., Andriantsitohaina, R., Muller, S., de La, R. G., Stoclet, J. C., and de Murcia, G. (1999) *EMBO J.* **18,** 4446-4454

51. Jagtap, P. and Szabo, C. (2005) *Nat. Rev. Drug Discov.* **4,** 421-440

52. Sarruf, D. A., Iankova, I., Abella, A., Assou, S., Miard, S., and Fajas, L. (2005) *Mol. Cell Biol.* **25,** 9985-9995

53. Boulias, K., Katrakili, N., Bamberg, K., Underhill, P., Greenfield, A., and Talianidis, I. (2005) *EMBO J.* **24,** 2624-2633

FOOTNOTES

We thank for Dr. Maria Malanga and Dr. Felix Althaus (Institute of Pharmacology and Toxicology, University of Zurich-Tierspital) for the siRNA sequence against PARP-2. The authors also acknowledge the help of Dr. Máté Demény, Dr. László Tora and Dr. Jean-Christophe Ame in the assays performed. This work was supported by grants of INSERM, Université Louis Pasteur, the European Union (LSHM-CT-2004-512013), NIH (DK 067320), FEBS (Long Term Fellowship), Centre National de la Recherche Scientifique, Association pour la Recherche contre le Cancer, Electricité de France, Ligue contre le Cancer, Commissariat à l'Energie Atomique and Agence Nationale pour la Recherche, Ambassade de la France en Hongrie, Bolyai Fellowship of the Hungarian Academy of Sciences to PB.

The abbreviations used are: WAT, white adipose tissue; PPAR, peroxisome proliferator-activated receptor; N-CoR, nuclear receptor corepressor; SRCs, steroid receptor coactivators; HDACs, histone deacetylases; PARP-2, poly(ADP-ribose) polymerase-2; PAR, poly(ADP-ribose) polymer; PARP-1, poly(ADP-ribose) polymerase-1; TTF1, thyroid transcription factor-1; WT, wild-type; TZD, troglitazone; FF, fenofibrate; MEHP, mono-ethyl-hexyl-phthalate Dex, dexamethasone; HE, haematoxylin-eosine; RT-qPCR, reverse transcription coupled quantitative PCR; LPL, lipoprotein lipase; FAS, fatty acid synthase; aP2, adipocyte fatty acid-binding protein 2; ERβ, estrogen receptor β; MMP-9, matrix metalloproteinase-9; K19, keratin-19; ChIP, chromatin immunoprecipitation; RXR, retinoid-X receptor; HEK 293, human embryonic kindey 293, HSL, hormone sensitive lipase; TNFα, tumor necrosis factor α.

The authors declare no conflict of interest.

FIGURE LEGENDS

Fig. 1. Abnormal WAT function in PARP-$2^{-/-}$ mice. A, Weight and macroscopic view of different adipose tissue depots in PARP-$2^{+/+}$ and PARP-$2^{-/-}$ mice (age of 7 months). In the PARP-$2^{-/-}$ mice there is a significant reduction of the different fat depots. Error bars represent +/- SEM. * $p<0.05$, ** $p<0.01$. B, The epididymal WAT stained with H&E (100X magnification). C, The arrow points towards a dilated capillary in the PARP-$2^{-/-}$ epididymal WAT (100X magnification, H&E). Staining with the F4/80 antibody detects macrophages (marked by #) in the vicinity of the dilated capillaries (*). D, Gene expression in epididymal WAT. * $p<0.05$

Fig. 2. Effect of PARP-2 on MEF differentiation into adipocytes. A, MEFs were differentiated into adipocytes and stained with Oil-Red O. On the terminally differentiated MEFs, Nile-red FACS analysis and lipid measurements were performed. The left histogram shows the percentage of differentiation as measured with Nile Red and the right histogram shows the accumulation of lipids in the culture. * $p<0.05$; ** $p<0.01$. B, Expression of selected marker genes of adipocyte differentiation as measured by RT-qPCR on MEF cDNA samples * $p<0.05$; ** $p<0.01$

Fig. 3. Characterisation of the pSuper-scrPARP-2 and the pSuper-siPARP-2 constructs. A, $3x10^7$ HEK cells were plated in Petri dishes and were BBS transfected on day 0 and on day 2. Cells were scraped from day 2 daily. These samples were analyzed by Western blotting. PARP-2 was depleted by the pSuper-siPARP-2 construct, but was unmodified by the pSuper-scrPARP-2 construct. Whereas the transfection with pBabe-PARP-2 resulted on day 3 and day 4 in a robust induction of PARP-2 expression, the transfection with pBabe alone did not modify PARP-2 expression.

Fig. 4. Effect of PARP-2 expression levels on PPARγ_2 transactivation. Effect of PARP-2 depletion and overexpression on the basal activity and receptor activation of PPARγ (A), PPARα (B), PPARβ (C) and ERβ (D) receptors. Error bars represent SD. ###, *** $p<0.001$; ** $p<0.01$; # $p<0.05$

Fig. 5. PPARγ_2 and PARP-2 occupy together the PPARγ-dependent promoters. A, PARP-2 is present on PPARγ driven promoters (aP2, CD36) as demonstrated in ChIP assays. The PARP-2 signal is increased in the PPARγ-driven promoters compared to the non-related, ERβ-driven K-19 promoter. Error bars represent SD. ###, *** $p<0.001$; #, * $p<0.05$. B, Similar ChIP assay was performed to compare the presence of PARP-2 on the promoters versus the coding sequence of the same gene. PARP-2 is present preferentially on the promoter rather then the coding sequence of the aP2 gene. Error bars represent SD. *** $p<0.001$; * $p<0.05$. C, As a positive control, the K19 primer set was tested for the ability to detect the presence of ERβ in ERβ transfected 3T3-L1 cells. The α-ERβ signal was significantly higher then the signal of the negative control α-MRE11 and the no antibody control. These data confirm that the K19 primer set is capable of the detection of the presence of the ERβ receptor on the K19 promoter. Error bars represent SD. ###, *** $p<0.001$; #, * $p<0.05$.

Table 1. Oligonucleotides used to generate pSuper-siPARP-2 and pSuper-scrPARP-2
The interfering sequences are in bold.

Name	**Sequence (5`-3`)**	**Structure**
siPARP-2 sense	GATCT**AAGATGATGCCCAGAGGAACT**TTCAAGAGA**AGTTCCTCTGGGCATCATCTT**TTTTTA	BglII/**sense**/loop/**antisense**/T(5)/Hind III
siPARP-2 antisense	AGCTTAAAAA**AAGATGATGCCCAGAGGAACT**TCTCTTGAA**AGTTCCTCTGGGCATCATCTT**A	HindIII/T(5)/**antisense**/loop/**sense**/Bgl II
scrPARP-2 sense	GATCT**TTCGGGGAACAAACGTGCAAC**TTCAAGAGA**GTTGCACGTTTGTTCCCCGAA**TTTTTA	BglII/**sense**/loop/**antisense**/T(5)/HindIII
scrPARP-2 antisense	AGCTTAAAAA**TTCGGGGAACAAACGTGCAAC**TCTCTTGAA**GTTGCACGTTTGTTCCCCGAA**A	HindIII/T(5)/**antisense**/loop/**sense**/BglII

Table 2. qPCR primers

Name	Sequence (5`-3`)	Accession number
Adiponectin	F 5`- AAG AAG GAC AAG GCC GTT CTC TT - 3` (652 - 674) R 5`- GCT ATG GGT AGT TGC AGT CAG TT – 3` (875 - 853)	NM_009605.4
aP2	F 5` - TGC CAC AAG GAA AGT GGC AG - 3` (132-151) R 5` - CTT CAC CTT CCT GTC GTC TG – 3` (294-275)	BC054426
CD36	F 5` - GAT GTG GAA CCC ATA ACT GGA TTC AC – 3` (1378 - 1403) R 5` - GGT CCC AGT CTC AAT TAG CCA CAG TA – 3` (1527 - 1502)	NM_007643
Cyclophylin B	F 5` - TGG AGA GCA CCA AGA CAG ACA – 3` (561 – 581) R 5` - TGC CGG AGT CGA CAA TGA T – 3` (626 - 608)	M60456
FAS	F 5` - GCT GCG GAA ACT TCA GGA AAT – 3` (6612 – 6632) R 5` - AGA GAC GTG TCA CTC CTG GAC TT – 3` (6695 – 6673)	BC046513
LPL	F 5` - AGG ACC CCT GAA GAC AC – 3` (317 – 333) R 5` - GGC ACC CAA CTC TCA TA – 3` (465 – 449)	BC003305
Leptin	F 5` - GAC ACC AAA ACC CTC AT – 3` (147 – 163) R 5` - CAG AGT CTG GTC CAT CT – 3` (296 – 280)	NM_008493
perilipin	F – 5` GCT TCT TCC GGC CCA GC – 3` (1511-1527) R – 5` CTC TTC TTG CGC AGC TGG CT – 3` (1580-1561)	NM_175640
PPARγ_1	F 5` - CCA CCA ACT TCG GAA TCA GCT – 3` (158 – 178) R 3` - TTT GTG GAT CCG GCA GTT AAG A – 3` (591 – 570)	NM_011146
PPARγ_2	F – 5` ATG GGTG AAA CTC TGG GAG ATT CT – 3` (46 – 69) R – 5` CTT GGA GCT TCA GGT CAT ATT TGT A – 3` (346 – 322)	AY243585
HSL	F - 5' CCT CAT GGC TCA ACT CC 3' (1633/2075 - 1649/2091) R - 5' GGT TCT TGA CTA TGG GTG A 3' (2067/2509 - 2049/2491)	NM_001039507.1/ NM_010719.5
TNFα	F – 5’ GCC ACC ACG CTC TTC TG 3’ (286-302) R – 3’ GGT GTG GGT GAG GAG CA 3’ (627-611)	NM_013693.2

Table 3. Chip primers

Name	Sequence	Reference
aP2	F 5`-CCC AGC AGG AAT CAG GTA GC-3` R 5`-AGA GGG CGG AGC AGT TCA TC-3`	(52)
CD36	F 5'-TTT GCT GGG ACA GAC CAA TC-3` R 5'-GCC ATG TTC CCA TCC AAG TA-3`	(53)
K19	F 5`- AAG GGT GGA GGT GTC TTG GT -3` R 5`- GCT TCT TTA CAC TCC TGC T AAA -3`	AF237661

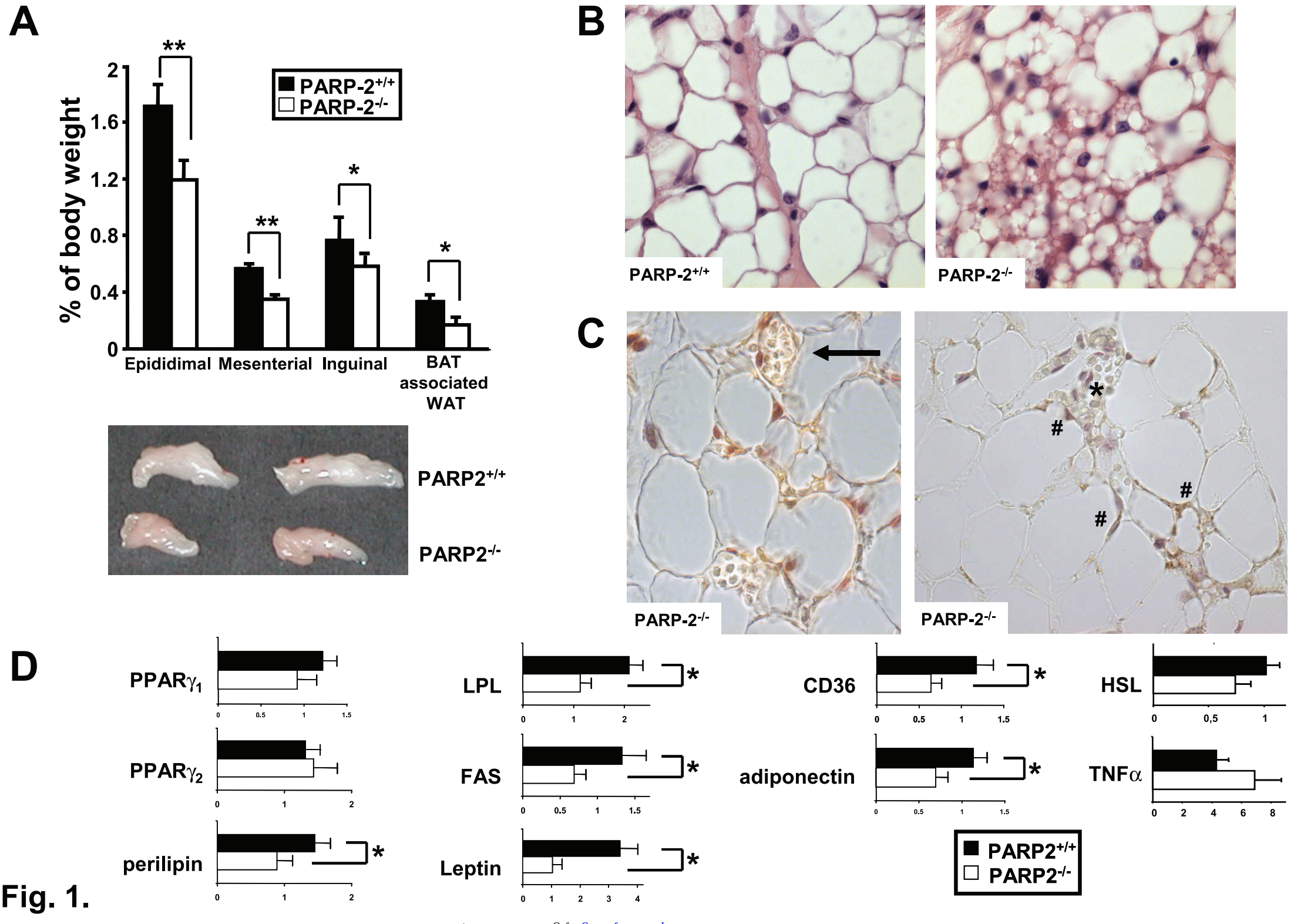
A
% of body weight
PARP-2+/+
PARP-2-/-
Epididimal
Mesenterial
Inguinal
BAT associated WAT
PARP2+/+
PARP2-/-
B
PARP-2+/+
PARP-2-/-
C
PARP-2-/-
PARP-2-/-
D
PPARγ1
PPARγ2
perilipin
LPL
FAS
Leptin
CD36
adiponectin
HSL
TNFα
PARP2+/+
PARP2-/-

Fig. 1.

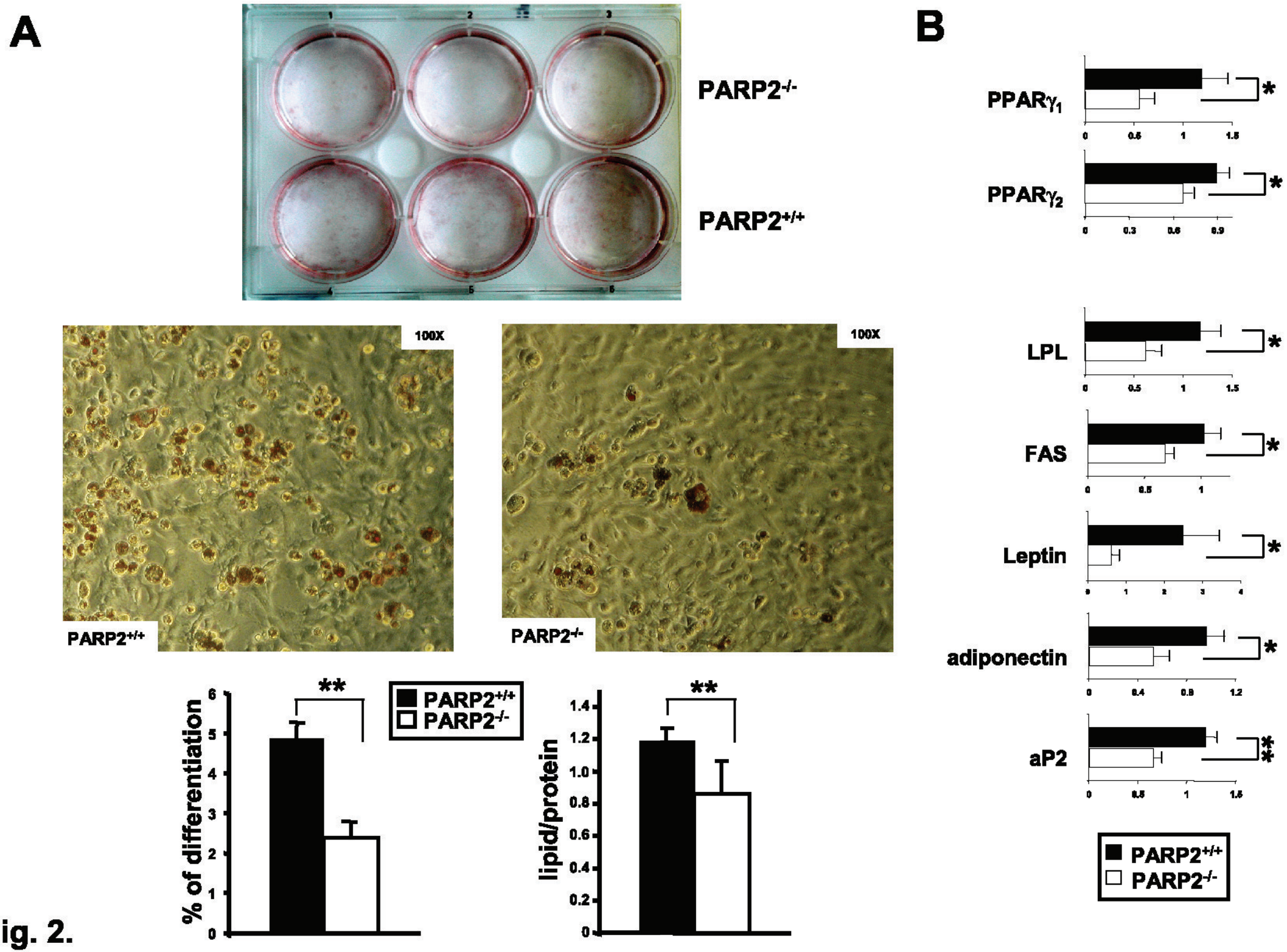
A
PARP2-/-
PARP2+/+
100X
PARP2+/+
100X
PARP2-/-
% of differentiation
**
PARP2+/+
PARP2-/-
lipid/protein
**
B
PPARγ1
PPARγ2
LPL
FAS
Leptin
adiponectin
aP2
PARP2+/+
PARP2-/-

Fig. 2.

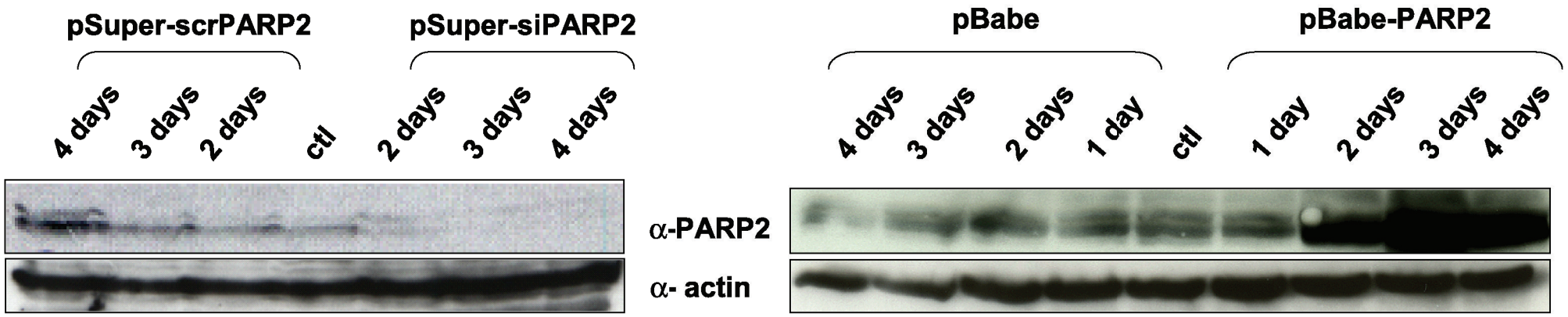
pSuper-scrPARP2
pSuper-siPARP2
pBabe
pBabe-PARP2
4 days
3 days
2 days
ctl
2 days
3 days
4 days
4 days
3 days
2 days
1 day
ctl
1 day
2 days
3 days
4 days
α-PARP2
α- actin

Fig. 3.

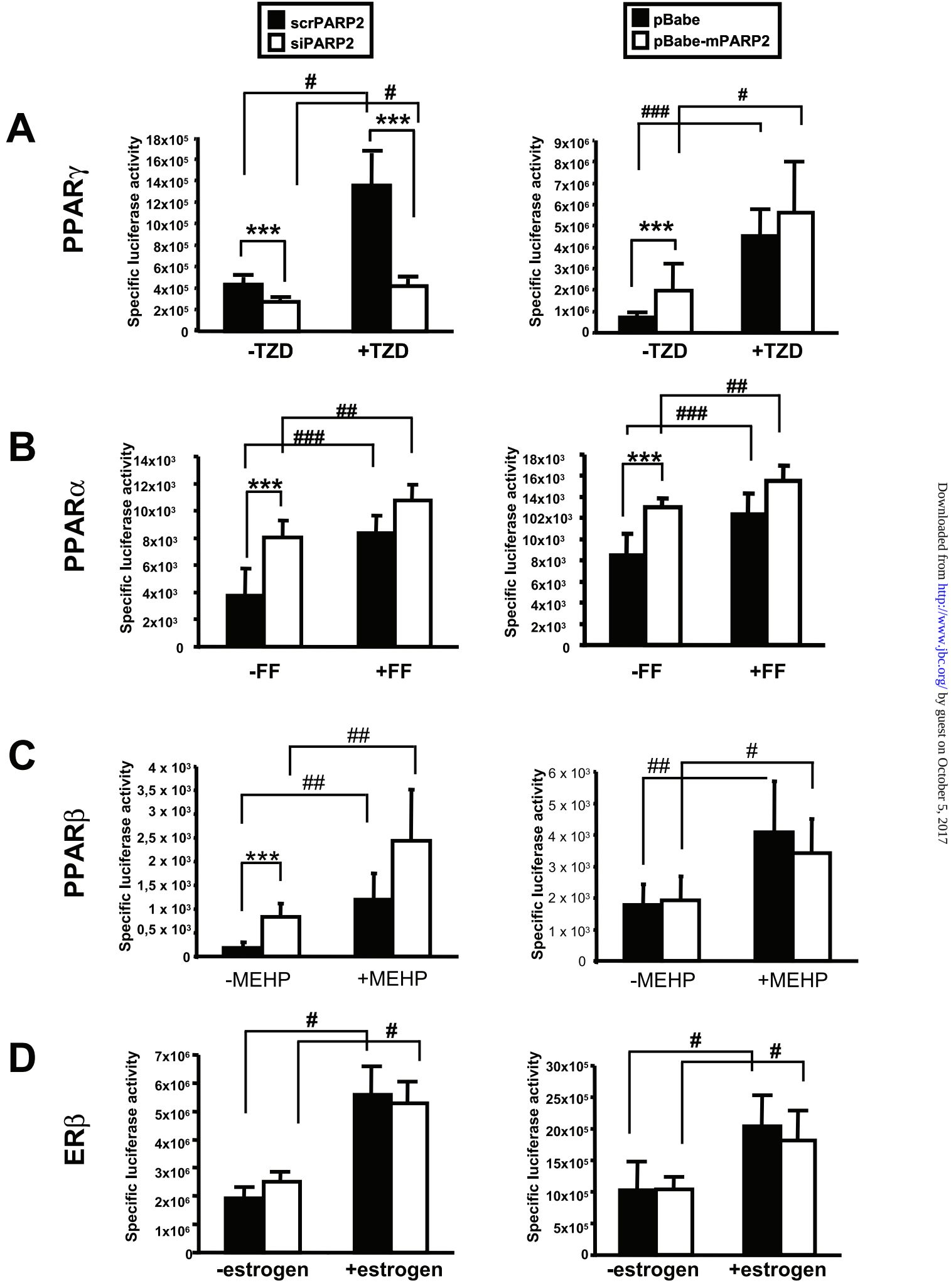

Fig. 4.

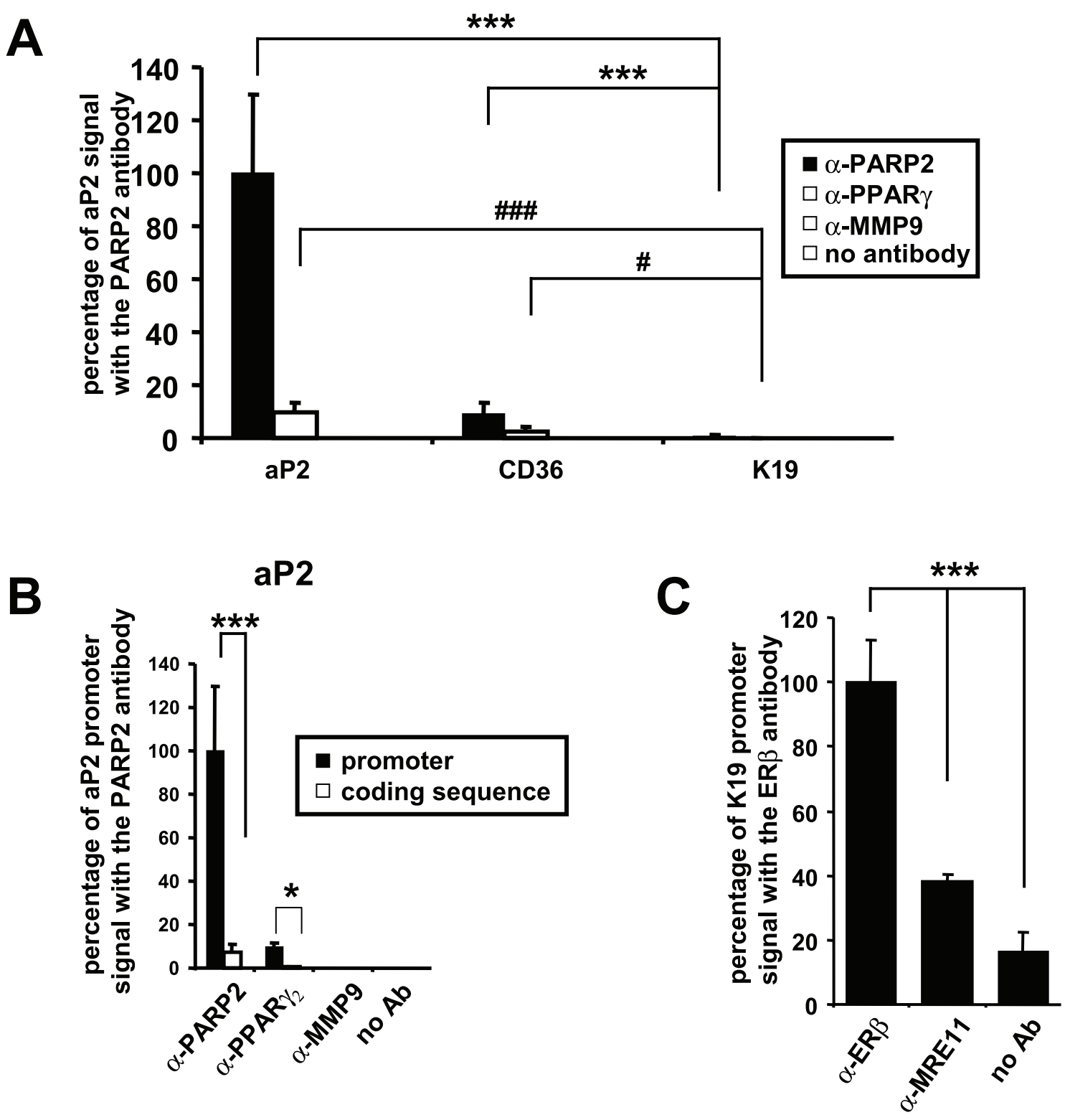
A
***
***
###
#
percentage of aP2 signal with the PARP2 antibody
140
120
100
80
60
40
20
0
aP2
CD36
K19
α-PARP2
α-PPARγ
α-MMP9
no antibody
B
aP2
***
*
percentage of aP2 promoter signal with the PARP2 antibody
promoter
coding sequence
α-PARP2
α-PPARγ2
α-MMP9
no Ab
C
***
percentage of K19 promoter signal with the ERβ antibody
120
100
80
60
40
20
0
α-ERβ
α-MRE11
no Ab

Fig. 5.

ADDITIONS AND CORRECTIONS

This paper is available online at www.jbc.org

THE JOURNAL OF BIOLOGICAL CHEMISTRY VOL. 283, NO. 9, p. 5972, February 29, 2008

VOLUME 282 (2007) PAGES 37738–37746

Poly(ADP-ribose) polymerase-2 controls adipocyte differentiation and adipose tissue function through the regulation of the activity of the retinoid X receptor/peroxisome proliferator-activated receptor-γ heterodimer.

Péter Bai, Sander M. Houten, Aline Huber, Valérie Schreiber, Mitsuhiro Watanabe, Borbála Kiss, Gilbert de Murcia, Johan Auwerx, and Josiane Ménissier-de Murcia

There was an error in the title of the article. The correct title is shown above.

VOLUME 283 (2008) PAGES 1653–1659

Novel binding site for Src Homology 2-containing protein-tyrosine phosphatase-1 in CD22 activated by B lymphocyte stimulation with antigen.

Chenghua Zhu, Motohiko Sato, Teruhiko Yanagisawa, Manabu Fujimoto, Takahiro Adachi, and Takeshi Tsubata

Dr. Adachi was inadvertently omitted as an author of this article. The correct authors are listed above. Dr. Adachi's affiliation is the Laboratory of Immunology, School of Biomedical Science, and the Department of Immunology, Medical Research Institute, Tokyo Medical and Dental University and Core Research for Evolutional Science and Technology, Japan Science and Technology Agency, 113-8510 Tokyo, Japan.

VOLUME 282 (2007) PAGES 23147–23162

The localization and activity of sphingosine kinase 1 are coordinately regulated with actin cytoskeletal dynamics in macrophages.

David J. Kusner, Christopher R. Thompson, Natalie A. Melrose, Stuart M. Pitson, Lina M. Obeid, and Shankar S. Iyer

On Page 23157, the final sentence of the legend to Fig. 8 should read as follows: Data represent the mean ± S.D. of duplicate determinations from a single representative experiment of a total of four identical experiments. On Page 23158, there is an error in the data in Fig. 9 (*A–C*), and these three panels should be retracted.

We suggest that subscribers photocopy these corrections and insert the photocopies in the original publication at the location of the original article. Authors are urged to introduce these corrections into any reprints they distribute. Secondary (abstract) services are urged to carry notice of these corrections as prominently as they carried the original abstracts.

PARP-2 controls adipocyte differentiation and adipose tissue function through the regulation of the activity of the RXR/PPAR γ heterodimer

Péter Bai, Sander M Houten, Aline Huber, Valérie Schreiber, Mitsuhiro Watanabe, Borbála Kiss, Gilbert de Murcia, Johan Auwerx and Josiane Ménissier-de Murcia

J. Biol. Chem. published online October 19, 2007
